

Response to Reviewers: Accounting for the photochemical variation of stratospheric NO₂ in the SAGE III/ISS solar occultation retrieval

Emmanuel Dekemper

Specific comments

1. On line 144, it is explained that the PRATMO model is not used above 40km in order to avoid unphysical values. This tends to indicate that the authors sought to use it on a larger vertical extent, but faced reliability issues. As a result, the disagreement between the two products (original SAGE-III NO₂ profiles, and those corrected for diurnal variability) tends to fade away as the altitude increases (Fig.6). As a note towards readers willing to apply the same correction technique, could you elaborate a bit on the reasons which forced you to not implement the diurnal correction above 40km? Is it due to the model itself? or to the specified O₃, pressure, and temperature profiles?... Was there any reliability concerns raised at lower altitudes?

The uncertainty in the SAGE measurements becomes greater than 20% above 40 km (and below 10 km) so we did not want to focus our results on these regions. In addition, the NO₂ concentration gets very low above 40 km. When calculating the scale factors we divide by the NO₂ at the tangent point altitude. For tangent points above ~40 km this results in dividing by a small number, which produces a large scale factor, despite the fact that the absolute difference in NO₂ might not be so large. This has been clarified in the manuscript.

2. It is not entirely clear if Fig.4, which shows the scaling factors applied to the path segment matrix X, shows an average scaling taking into account the two disymmetric sides of the light path, or if it only shows the factors for one half of the path. In the latter case, which half is it? Could you make it a bit clearer in your description?

This figure shows the scale factors from either side of the tangent point added together. This information has been added to the figure caption.

3. On page 10, the authors point out that the agreement of the improved NO₂ profiles is better at sunrise than sunset. The discussion about this difference is somewhat vague, especially that, to my knowledge, OSIRIS is sounding the atmosphere both close to local sunset and sunrise. Could this topic be slightly expanded? For instance by listing the possible reasons for this pending bias. In particular, did you consider to restrict the coincidence criteria to less than 24 hours, in order to limit the time gap which needs to be solved by the PRATMO model?

We only use the morning OSIRIS measurements (ascending node). A drift in the OSIRIS orbit resulted in many of the descending measurements occurring at night, when OSIRIS cannot measure, which affects the sampling. Because of this, it is common to use only the morning OSIRIS data. Using coincidence criteria of less than 24 hours did not result in large differences in the comparisons so we chose to have more data points in each bin. This has been clarified in the manuscript.

Technical corrections

4. Line 52: double "the" **Fixed**

5. Line 221: "... between with ..." should read "... with ..." **Fixed**

Referee #2

Specific comments

Line 8: What is “undoing” a retrieval? Reversing the algorithm to back out optical depth?

Yes, by undoing a retrieval we mean converting the number densities back to optical depths. This has been clarified in the text.

Line 102 and Fig. 2 caption: Which dashed line? There are 2. Maybe draw the SZA on the figure.

Both dashed lines. More detail has been added to the Figure and the text so that this is better explained.

Line 146: The text states: “The values in the figure are not multiplied by the path lengths”. Would we expect them to be?

The matrix used in the retrieval generally consists only of path length elements. For the diurnally varying retrieval we are multiplying each path length by a corresponding scale factor. The figure only shows these scale factor values, as opposed to the final matrix (including path lengths) that is used to do the retrieval. So we thought it useful to clarify that this Figure only considers the scale factors that go into the final path length matrix.

Line 170: Please elaborate on how the bias is not consistent with the differences.

Figure 1 shows that the shape of the diurnal cycle across the terminator is different at sunrise and sunset, which results in different photochemical scale factors. A comment has been added to the manuscript.

Fig. 6: A panel showing percent difference would be helpful as well.

A panel showing the percent difference has been added to the figure.

Fig. 7: Is there bad data in the middle panel of the bottom row?

Yes, there were a few bad data points. The figure has been changed to only include NO₂ values within five standard deviations of the mean.

Fig. 9a: It appears that while the negative bias is reduced in the SAGE_{dv} case, the positive biases at lower altitudes increase. This merits some discussion.

This is discussed in lines 204-207 (210-213 in updated manuscript). The positive biases increase because the diurnal effect is very large near the tropical tropopause and the absolute NO₂ values are low, resulting in a decrease in the diurnally varying SAGE III/ISS NO₂ that is greater than the initial difference between SAGE III/ISS and OSIRIS NO₂.

Fig. 9: Are the right (b) panels SAGE_{dv} – SAGE, or (OSIRIS-SAGE_{dv}) – (OSIRIS-SAGE)?

In other words, why is “SAGE_{dv} – SAGE” positive when it is stated that “neglect of diurnal variations in the SAGE v5.1 retrieval always biases the results high”? Figure 9 might be more intuitive if it were presented as SAGE – OSIRIS rather than OSIRIS – SAGE.

The right panels are indeed the difference $(OSIRIS - SAGE_{dv}) - (OSIRIS - SAGE)$. This has been clarified in the figure. The figure has also been changed to show the difference $SAGE - OSIRIS$ instead of $OSIRIS - SAGE$.

Accounting for the photochemical variation of stratospheric NO₂ in the SAGE III/ISS solar occultation retrieval

Kimberlee Dubé¹, Adam Bourassa¹, Daniel Zawada¹, Douglas Degenstein¹, Robert Damadeo², David Flittner², and William Randel³

¹Institute of Space and Atmospheric Studies, University of Saskatchewan, Saskatchewan, Canada

²NASA Langley Research Center, Hampton, VA, USA

³National Center for Atmospheric Research, Boulder, CO, USA

Correspondence: Kimberlee Dubé (kimberlee.dube@usask.ca)

Abstract. The Stratospheric Aerosol and Gas Experiment (SAGE) III has been operating on the International Space Station (ISS) since mid 2017. Nitrogen dioxide (NO₂) number density profiles are routinely retrieved from SAGE III/ISS solar occultation measurements in the middle atmosphere. Although NO₂ density varies throughout the day due to photochemistry, the standard SAGE NO₂ retrieval algorithm neglects these variations along the instrument's line of sight by assuming that the number density has a constant gradient within a given vertical layer of the atmosphere. This assumption will result in a retrieval bias for a species like NO₂ that changes rapidly across the terminator. In this work we account for diurnal variations in retrievals of NO₂ from the SAGE III/ISS measurements, and determine the impact of this algorithm improvement on the resulting NO₂ number densities. The [first step in applying the](#) diurnal correction is ~~applied by first undoing the SAGE III/ISS retrieval using to use~~ publicly available SAGE III/ISS products to ~~obtain an optical depth profile~~[convert the retrieved number density profiles to optical depth profiles](#). The retrieval is then ~~performed re-performed~~ with a new matrix that applies photochemical scale factors for each point along the line of sight according to the changing solar zenith angle. In general NO₂ that is retrieved by accounting for these diurnal variations is more than 10% lower than the standard algorithm below 30 km. This effect is greatest in winter at high latitudes, and generally greater for sunrise occultations than sunset. Comparisons with coincident profiles from the Optical Spectrograph and InfraRed Imager System (OSIRIS) show that NO₂ from SAGE III/ISS is generally biased high, however the agreement improves by up to 20% in the mid stratosphere when diurnal variations are accounted for in the retrieval. We conclude that diurnal variations along the SAGE III/ISS line of sight are an important term to consider for NO₂ analyses at altitudes below 30 km.

Copyright statement. TEXT

1 Introduction

20 The Stratospheric Aerosol and Gas Experiment (SAGE) III on the International Space Station (ISS) uses solar occultation to measure the attenuation of sunlight through the middle atmosphere (Cisewski et al., 2014). These measurements are used

to retrieve vertical profiles of nitrogen dioxide (NO_2), as well as other atmospheric constituents, mainly ozone and aerosol extinction coefficients. The SAGE III/ISS data complements that from the earlier SAGE II (McCormick, 1987) and SAGE III/Meteor-3M missions (Mauldin III et al., 1998), as well as data from limb-viewing instruments such as the Optical Spectro-
25 graph and Infrared Imager System (OSIRIS, Llewellyn et al., 2004), to provide a long-term record of NO_2 . It is important to have these data sets for understanding trends and variability in the stratosphere as NO_2 plays a role in the chemical depletion of the ozone layer. Several studies of the long-term trends and variability in NO_2 (Randel et al., 1999; Liley et al., 2000; Park et al., 2017; Galytska et al., 2019; Dubé et al., 2020) have shown a consistent increase in NO_2 and an associated decrease in O_3 .

30 NO_2 is mainly destroyed by photolysis so the concentration, or density, of NO_2 that is measured depends greatly on the position of the sun: there is a rapid decrease in NO_2 at sunrise and a rapid increase at sunset. During solar occultation measurements, such as those taken by SAGE III/ISS, the solar zenith angle (SZA) is 90° at the tangent point, but varies along the instrument's line of sight (LOS). The retrieved NO_2 profile has contributions from the full LOS, so it includes contributions from both the day and night sides of the Earth, which can have substantially different amounts of NO_2 . The existing SAGE
35 III/ISS retrieval neglects variations in SZA along the LOS by assuming the concentration of NO_2 has a constant gradient at each altitude above the Earth's surface (SAGE III Algorithm Theoretical Basis Document, 2002). This is a source of systematic uncertainty in the retrieved NO_2 that has not been quantified for SAGE III/ISS. Previous studies have examined the effect of this variation in SZA on NO_2 retrieved from other occultation instruments and showed that ignoring it can result in a high bias, especially below 25 km (Gordley et al., 1996; Newchurch et al., 1996; Brohede et al., 2007). The purpose of this work
40 is to account for diurnal variations along the LOS, assess the impact, and provide an improved SAGE III/ISS NO_2 data set for further study. This is done by adding correction factors to the retrieval that account for variations in NO_2 due to changing solar zenith angle along the LOS. By comparing the NO_2 concentration from this improved retrieval to that from the existing SAGE III/ISS retrieval it is possible to determine the importance of the photochemical effect. The results are also compared to NO_2 retrievals from OSIRIS limb scattering measurements to determine how the photochemical correction changes the bias
45 between NO_2 products from the two different instruments.

2 NO_2 Photochemistry

The NO_2 number density depends on local solar time (LST) and equivalently, SZA (Figure 1). There is a sharp decrease in the NO_2 concentration at sunrise as NO_2 is photolyzed to become NO. Throughout the daylight hours NO_2 and NO are in approximate equilibrium. At sunset NO production ceases, resulting in a rapid increase in NO_2 . Overnight NO_2 decreases more
50 slowly as it is converted to nitrogen-containing reservoir species. The exact shape of this diurnal cycle depends on altitude: the NO_2 concentration at 40 km stays roughly constant during the day and night, while at altitudes with more NO_2 there is a steady increase during the day and decrease at night.

The values in Figure 1 were calculated with the ~~the~~ photochemical box model originally developed by Prather et al., 1992, which has been successively updated and is now often referred to as PRATMO (McLinden et al., 2000; Adams et al., 2017).

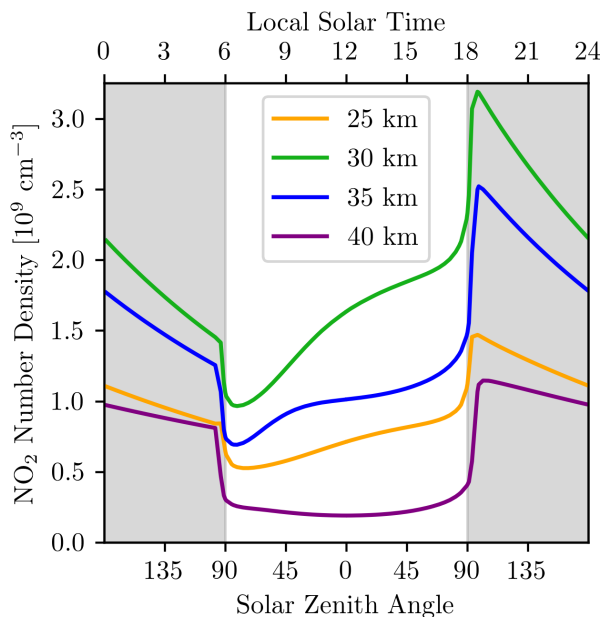


Figure 1. Daily cycle in NO_2 at the equator as a function of local solar time (top axis) and solar zenith angle (bottom axis) for four altitudes. NO_2 number density calculated with PRATMO photochemical box model.

55 PRATMO takes an input atmospheric state consisting of specified ozone, temperature, pressure, and air density profiles for a set latitude, longitude, and date. These input parameters are kept constant. The model then calculates a set of chemical reactions over a single day, iterating until the start and end values converge (Prather, 1992). This results in a 24 hour steady-state system of each species in the model. The model outputs are the NO_2 profiles at any predetermined SZAs. These values can be used to scale the measured NO_2 to different solar times in order to account for variations in SZA along the measurement LOS (Section

60 4). PRATMO scaling was used in several previous studies (e.g. Adams et al., 2017; Park et al., 2017; Dubé et al., 2020) to compare NO_2 from instruments that measure at different times of day.

3 Instruments

3.1 SAGE III/ISS

SAGE III has been in orbit on the ISS since March 2017. Level 2 data are available from June 2017 onwards. The ISS has an

65 inclination of 51.6° , allowing SAGE III/ISS to view latitudes from 70°N to 70°S . The CCD spectrometer is configurable and currently observes wavelengths between $\sim 280\text{nm}$ and $\sim 1035\text{nm}$ with a resolution of 1-2nm. A separate photodiode covers $\sim 1542\text{nm} \pm 15\text{nm}$. During each occultation SAGE III/ISS continuously scans back and forth across the sun to measure the irradiance. There are 15 sunrise and 15 sunset events per day. The coverage of SAGE III/ISS is very similar to that of SAGE

70 II. The sunrise and sunset measurements progress in opposing directions, with each requiring about one month to achieve near global coverage.

The irradiances are used in the standard SAGE III/ISS retrieval (version 5.1, SAGE III Algorithm Theoretical Basis Document, 2002) to determine the number density of several species, as well as the aerosol extinction at several wavelengths. The first step in the algorithm is to calculate slant path transmission profiles for each wavelength channel from the measured irradiance. Each slant path transmission profile is converted to a slant path optical depth profile that contains contributions
75 from Rayleigh scattering, aerosol extinction, and absorption by at least one species. With this information NO_2 and O_3 slant path number density profiles are solved for simultaneously using multiple linear regression. NO_2 is retrieved from channel S3, covering 433 to 450 nm. The slant path number density is converted to vertical number density profiles using a global fit method that assumes each layer of the atmosphere is a spherical shell with a constant gradient. The final NO_2 number density is available from 10 to 45 km on a 0.5 km grid with a vertical resolution of about 1.5 km. The reported uncertainty in the SAGE
80 III/ISS NO_2 is around 5% at 30 km, and increases to up to 20% at 10 km and 40 km. This uncertainty is due to measurement noise only, and does not account for systematic bias due to the horizontal homogeneity assumption.

3.2 OSIRIS

OSIRIS has been in sun-synchronous orbit on the Odin satellite since October 2001 (Murtagh et al., 2002; Llewellyn et al., 2004). There are 100 to 400 vertical profiles of limb-scattered solar irradiance measured each day, at wavelengths from 280 to
85 800 nm. NO_2 is retrieved by spectral fitting in the wavelength range from 435 to 477 nm for altitudes from the cloud top to 39.5 km with a resolution of 2 km.

Earlier versions of the OSIRIS NO_2 retrieval were developed by Haley et al. (2004), Bourassa et al. (2011), and Sioris et al. (2017). The most recent data, version 7.0, is used here for validation of SAGE III/ISS NO_2 . Version 7.0 improves upon version 6.0 by using solar Fraunhofer lines to fit the spectral point spread function of OSIRIS rather than using pre-flight calibration
90 values. Cloud and aerosol discrimination is also refined to better detect cloudy scenes and to push the retrieval farther into the UTLS ([Upper Troposphere Lower Stratosphere](#)) following the method of Rieger et al. (2019).

The OSIRIS LOS is approximately aligned with the terminator so the variation in SZA along the LOS is much smaller than for occultation instruments. McLinden et al. (2006) studied the effect of the diurnal error on NO_2 from OSIRIS and found that it is only significant when the SZA is near 90° and the solar azimuth angle varies significantly from 90° . These extreme
95 conditions occurred in 16% of profiles from 2004, resulting in errors of up to 35% in the OSIRIS NO_2 below 25 km. Sioris et al. (2017) used PRATMO to create a 2D OSIRIS NO_2 retrieval to further assess the impact of diurnal variations on the results. They found minimally improved agreement between OSIRIS NO_2 and NO_2 from balloon measurements, particularly below 20 km. Owing to the minimal effect for OSIRIS, the standard NO_2 data product is produced neglecting the NO_2 photochemical gradient.

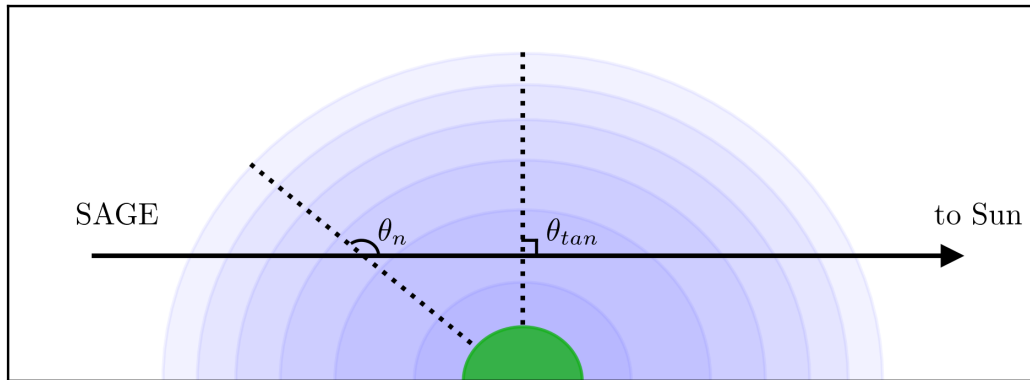


Figure 2. Geometry of a SAGE III occultation. The green semi-circle represents the Earth, and the blue semi-circles represent layers of the atmosphere. The angle between θ_{tan} is the dashed-line SZA at the tangent point, and solid-line the angle θ_n is the solar-zenith SZA angle at for a given location shell at altitude n .

100 4 Retrieval

During each occultation SAGE III/ISS looks through multiple layers of the atmosphere, called shells. Each shell is defined by its altitude. Figure 2 illustrates this geometry. The black arrow represents the LOS, pointing from the instrument to the sun. The SZA at a given location is the angle between the dashed-dotted line and the LOS. At the tangent point this angle, θ_{tan} is 90° . For some other shell with an altitude n the SZA θ_n is greater than 90° on the instrument side of the tangent point, as shown in the Figure. For this same shell altitude the SZA is less than 90° on the sun side of the tangent point.

The SAGE III/ISS retrieval assumes that the number density of each chemical constituent is either constant or has a constant gradient within a shell (SAGE III Algorithm Theoretical Basis Document, 2002). This assumption is generally valid for species such as ozone that undergo minimal diurnal variation in the stratosphere, however it is not true for NO_2 . This can be understood by considering Figure 3. For both lines of sight in the figure the SZA at the tangent point is 90° . To retrieve the NO_2 concentration at the tangent point of a given LOS we need to know the NO_2 concentration at each shell altitude that the LOS passes through. For example, the retrieved NO_2 at 22 km depends on the NO_2 at 32 km. The NO_2 at 32 km is retrieved at the tangent point, where the SZA is 90° , but the 22 km line of sight passes through the 32 km shell when the SZA is around 86.8° on the near side of the tangent point and 93.2° on the far side (left panel of Figure 3). The right panel of Figure 3 shows that the NO_2 concentration at 32 km and the two SZAs where the 22 km LOS passes through that shell are both different from the concentration when the SZA is 90° . In addition, the NO_2 does not change linearly across the terminator so deviations from linearity on either side of the LOS do not cancel out. Therefore using the 32 km NO_2 at 90° to retrieve the 22 km NO_2 is inaccurate, and it cannot be assumed that the number density has a constant gradient across the terminator within a layer of the atmosphere when performing the retrieval. This lack of spherical homogeneity can be accounted for by adding factors to the retrieval that scale the NO_2 according to SZA, at each location along the LOS.

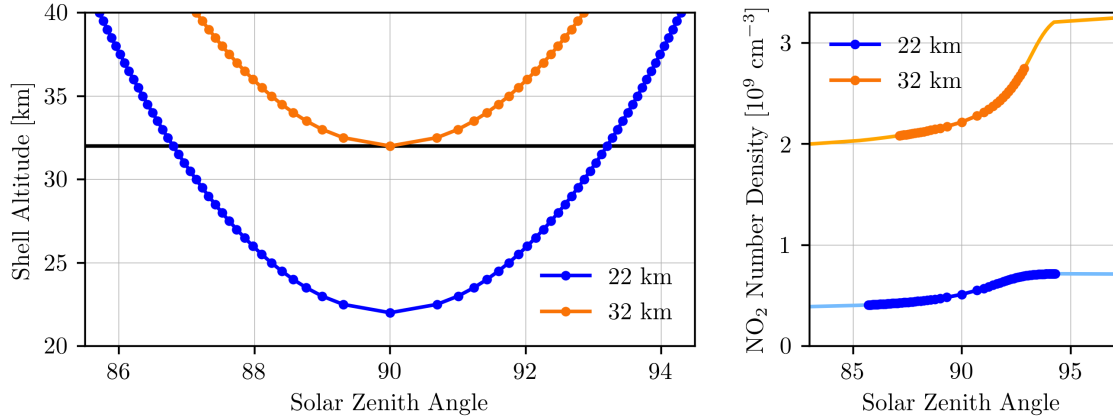


Figure 3. Left: Change in SZA with shell altitude along two lines of sight for a simulated sunset occultation. Right: Change in NO₂ at tangent altitudes of 22 km and 32 km for the same simulated sunset occultation. The dark, dotted lines correspond to the lines of sight from the left panel.

120 Ideally we would incorporate the scale factors by redoing the conversion of slant path optical depth, obtained directly from the solar transmission measurements, to number density. As the SAGE III/ISS NO₂ optical depth profiles are not publicly available, we instead start by undoing the SAGE III/ISS retrieval to revert the number densities to optical depths. This is done using the matrix equation,

$$\tau = \sigma X_0 n_0, \tag{1}$$

125 where τ is the vertical profile of slant path optical depths from NO₂, σ is the NO₂ cross section, and n_0 is the number density profile. X_0 is the path length matrix where each row represents a LOS for a particular tangent point altitude and each column represents a different altitude through which the LOS passes. Each element of X_0 is the path length distance between subsequent shells along the LOS. The path lengths on opposite sides of the tangent point are the same (i.e. the distance from shell 1 to 2 on the instrument side of the tangent point is the same as the distance from shell 1 to 2 on the sun side) which
 130 allows X_0 to be written as an upper triangular matrix where values from opposite sides of the tangent point are added together.

These optical depths are used to find the number densities accounting for diurnal variations, n_{dv} , using a new matrix, X_{dv} ,

$$n_{dv} = \sigma^{-1} X_{dv}^{-1} \tau. \tag{2}$$

In this matrix each path length includes a factor, explained below, that depends on the SZA at that location. Note that the NO₂ cross section is the same in both equations 1 and 2 and so it cancels out when finding n_{dv} . Although this is not strictly the
 135 case, using a constant cross section is a reasonable approximation as the cross section has a weak temperature and pressure dependence. The equations also assume that optical depth is constant within each layer of the atmosphere.

For a given SAGE III/ISS scan we know the date and time, the tangent point position, the spacecraft position, and the NO₂ number density from the SAGE v5.1 retrieval. This information is all that is needed to construct X_0 . To build the matrix we

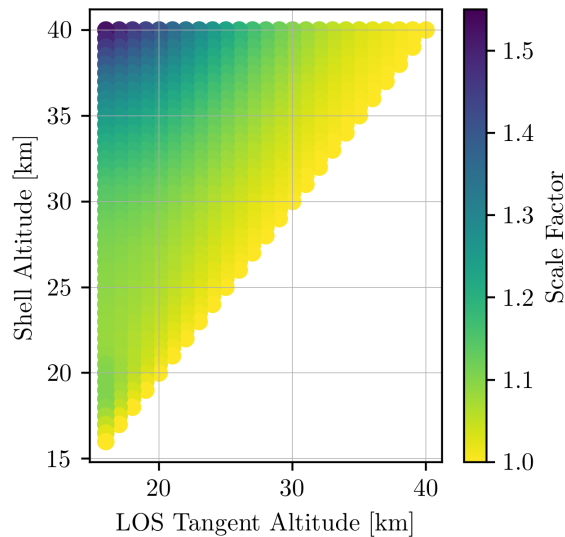


Figure 4. Scale factor matrix for a sunset occultation at the equator in March, simulated with PRATMO. The scale factors from either side of the tangent point are added to together, resulting in an upper triangular matrix.

iterate through each LOS, moving from the tangent point to the top of the atmosphere. The LOS is the vector from the satellite
 140 to the tangent point. The effect of refraction is neglected as it is small at the altitudes being considered.

The LOS for a particular tangent altitude intersects all of the shells above it. To find the scale factors for a given LOS we
 first find the apparent local solar time at the midpoint of each path created by the intersection of that LOS with the shells.
 PRATMO is then run with input ozone, temperature, and pressure from the SAGE III/ISS Level 2 scan data. The model NO₂
 is computed at each calculated LST and at a SZA of 90°, corresponding to the exact time of sunrise or sunset. For each shell
 145 altitude along the LOS, the scale factor is the PRATMO NO₂ at that altitude (corresponding to the LST at that location) divided
 by the PRATMO NO₂ at the tangent point altitude for that LOS (the scale factor is 1 for the shell containing the tangent point).
 There is no scaling done above 40 km as the low amount of NO₂ can lead to ~~unphysical scale factors~~ unphysically large scale
 factors, despite small absolute differences in NO₂ along the LOS. The uncertainty in the SAGE III/ISS NO₂ also becomes
 large above 40 km and we want to prevent abnormal values from influencing the results at lower altitudes.

150 Figure 4 shows the photochemical scale factor matrix for a simulated event. The values in the figure are not multiplied by
 the path lengths. The matrix is created such that the scale factors from opposite sides of the tangent point need to be added
 together. This results in a scale factor that is equal to one along the diagonal, corresponding to unscaled values at the tangent
 point, and greater than one everywhere else. The scale factors increase as the path length component of the LOS gets further
 away from the tangent point.

155 It is also useful to look at the scale factor as a function of altitude along each LOS (Figure 5). Lower lines of sight pass
 through more layers of the atmosphere, resulting in greater scale factors. For lines of sight below about 30 km the change
 in scale factor with altitude becomes non-linear. This is because the shape of NO₂ cycle across the terminator changes with

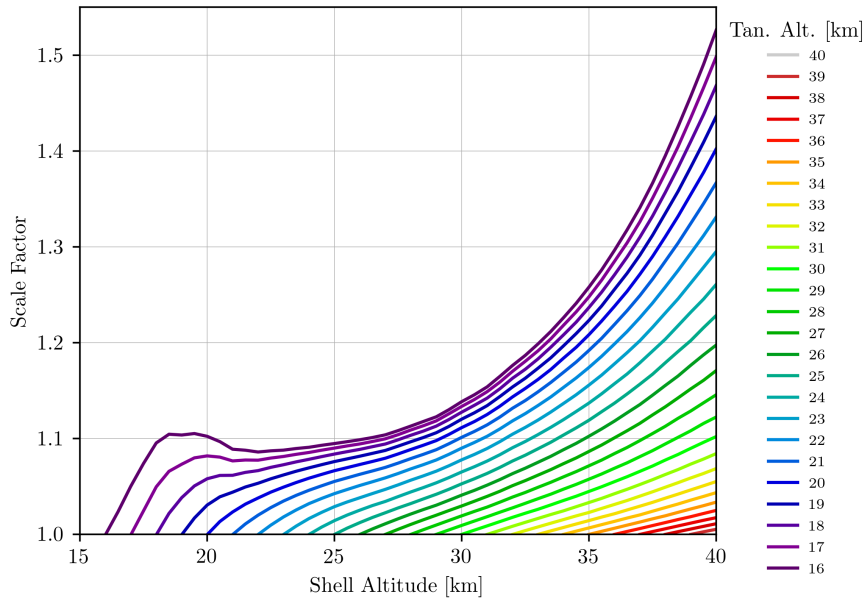


Figure 5. Scale factors along each line of sight for a sunset occultation at the equator in March, simulated with PRATMO.

altitude (right panel of Figure 3). At higher altitudes the NO_2 increases along the whole LOS; below about 30 km the NO_2 starts to level out on the night-side (the curve on either side of the terminator becomes different), changing the slope of the scale factor curves in Figure 5.

The scaled path length matrix, X_{dv} , is equal to the initial path length matrix, X_0 , where each element has been multiplied by the corresponding element from the scale factor matrix shown in Figure 4. X_{dv} is used along with the calculated slant path optical depths in Equation 2 to get the NO_2 number density, accounting for diurnal variations. The resulting values of n_{dv} will be smaller than the original retrieved values. This is because the gradient on the near side of the LOS is smaller than the gradient on the far side, resulting in scale factors greater than one and therefore lower NO_2 . Figure 6 shows the results for a sample SAGE III/ISS event. The left panel contains the optical depth profile, while the right-center panel compares the SAGE III/ISS NO_2 number density with the diurnally varying number density. In general the, and the right panel shows the percent difference between the two number density profiles. For this SAGE III/ISS event the percent difference between the two profiles becomes greater as altitude decreases to 17 km. Below this point the difference starts to become smaller again.

170 5 Results

The effect of accounting for diurnal variations on the retrieved SAGE III/ISS NO_2 is quantified by the difference between the SAGE v5.1 retrieval and the diurnally varying retrieval (Figure 7). In general the difference between the retrievals becomes greater than 20% below 25 km, which is larger than the reported random uncertainty in the SAGE III/ISS NO_2 . Including the diurnal variations is more important in the winter at high latitudes; at these times the relative NO_2 decrease at sunrise/increase

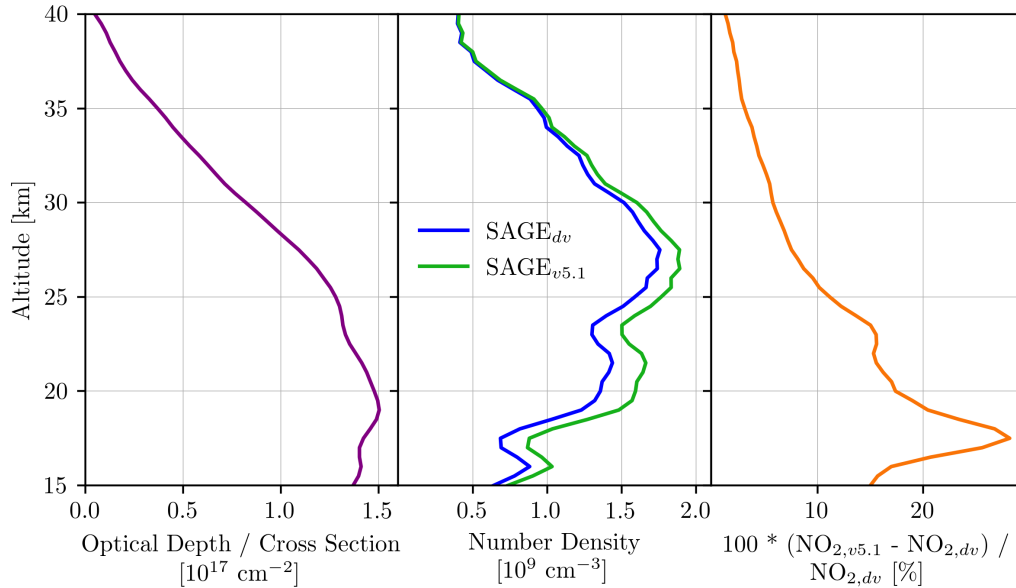


Figure 6. Optical Left: NO_2 optical depth and Centre: NO_2 number density for both the diurnally varying and SAGE v5.1 retrievals. Right: Percent difference between the two number density profiles. Calculated for SAGE III/ISS event 967110.

175 at sunset is larger. The bias between the retrievals is not consistent between the sunrise and sunset NO_2 due to the differences in NO_2 chemistry at these times. This can be seen by looking at Figure 1: the change in NO_2 across the terminator has a different shape at sunrise than at sunset. Including diurnal variations along the LOS in the retrieval has a greater effect on sunrise than sunset above 25 km in the tropics and everywhere at higher latitudes.

The results presented in Figure 7 are very similar to those in Brohede et al. (2007), where they estimated the magnitude of neglecting diurnal variations in NO_2 for a simulated occultation instrument (not specific to SAGE II or III). They found that the bias increases rapidly below 25 km (below the peak in NO_2 density) and is larger at low latitudes for sunset. They also found that at high latitudes the bias is largest near equinoxes and sunrise values are slightly larger than sunset values. It was determined that this effect was enough to explain most of the difference between SAGE III/Meteor-3M and OSIRIS NO_2 at low altitudes (although they did not actually apply the correction to the SAGE III/Meteor-3M data).

185 The magnitude of the photochemical effect is also similar to that used in the Halogen Occultation Experiment (HALOE, Russell III et al., 1993) retrieval. HALOE is one occultation instrument that does include diurnal effects in the retrieval (Gordley et al., 1996). They use a factor based on results from the previous layer and a model that provides the NO_2 mixing ratio as a function of SZA and season. This is less accurate than the scale factors used in the present study, which are modelled for each NO_2 profile individually. The effect of the HALOE scaling is considered significant below 25 hPa (≈ 27 km). They also

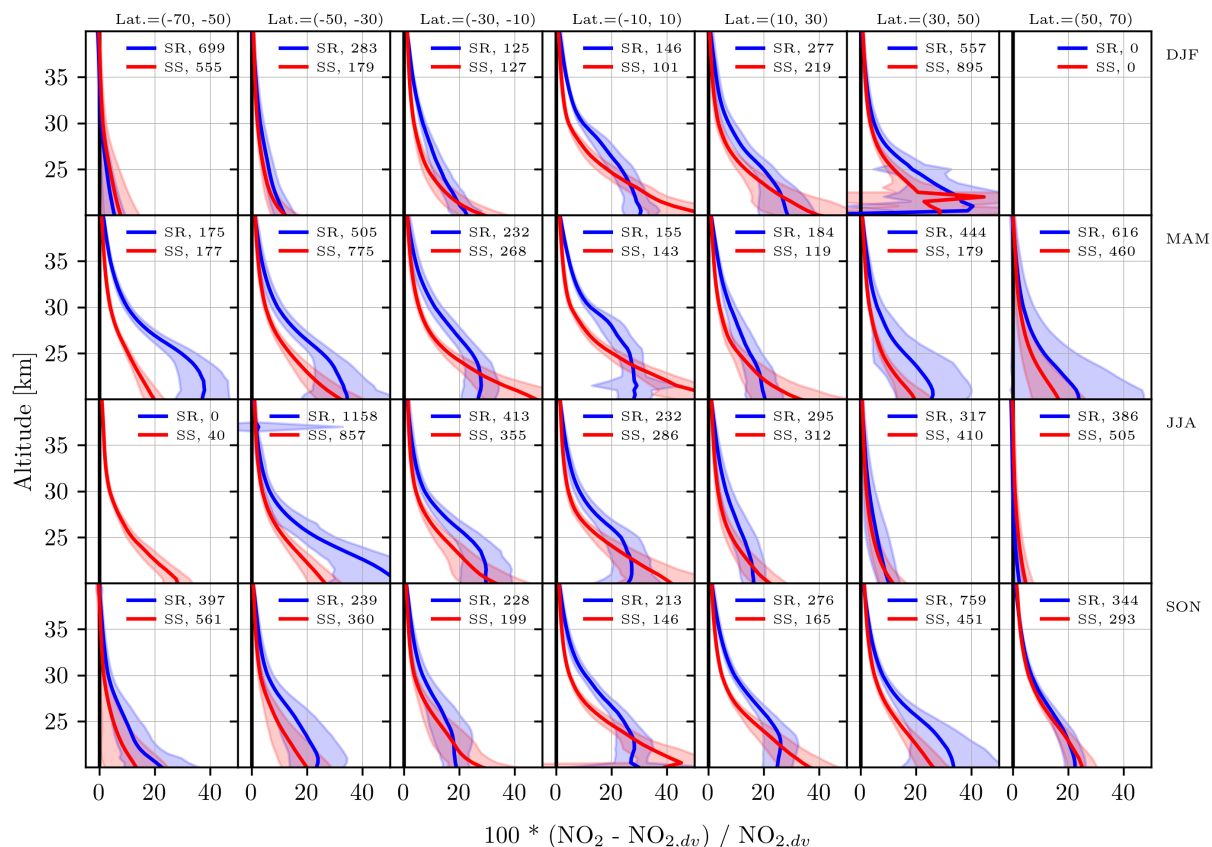


Figure 7. Mean difference between the SAGE v5.1 and diurnally varying (dv) retrievals for SAGE III/ISS sunset and sunrise NO₂. The error bars are the standard deviation. NO₂ [values more than five standard deviations from the mean are not included.](#)

190 found the diurnal effect in sunrise to be 2-3 times larger than in sunset, which is greater than the difference between sunrise and sunset observed here for SAGE III/ISS.

Accounting for diurnal variations in the retrieval changes the SAGE III/ISS NO₂ time series. This is shown in Figure 8 for several latitude bins at 25.5 km. The sunset NO₂ number density decreases by about 5% to 20%, with the largest decreases occurring in the tropics. The effect of the diurnal variations on the sunrise NO₂ has a more pronounced seasonal cycle than
 195 sunset, with a greater decrease in the winter, and a difference ranging from 5% to 30%. During winter months the diurnal effect is about 2 times greater at sunrise than at sunset, which is comparable to the difference reported for HALOE NO₂ in Gordley et al. (1996). However during the summer the bias is similar for both sunrise and sunset. These variations in the time series should be considered when using the SAGE III/ISS NO₂ data.

Both the diurnally varying and SAGE v5.1 retrievals were compared with OSIRIS NO₂ as a way to validate the data (panel
 200 a of Figure 9). [Only the morning \(ascending node\) OSIRIS measurements are used as a drift in the OSIRIS orbit affects the descending node sampling.](#) The comparisons were done for events within 24 hours, 10° longitude, and 2° latitude, although

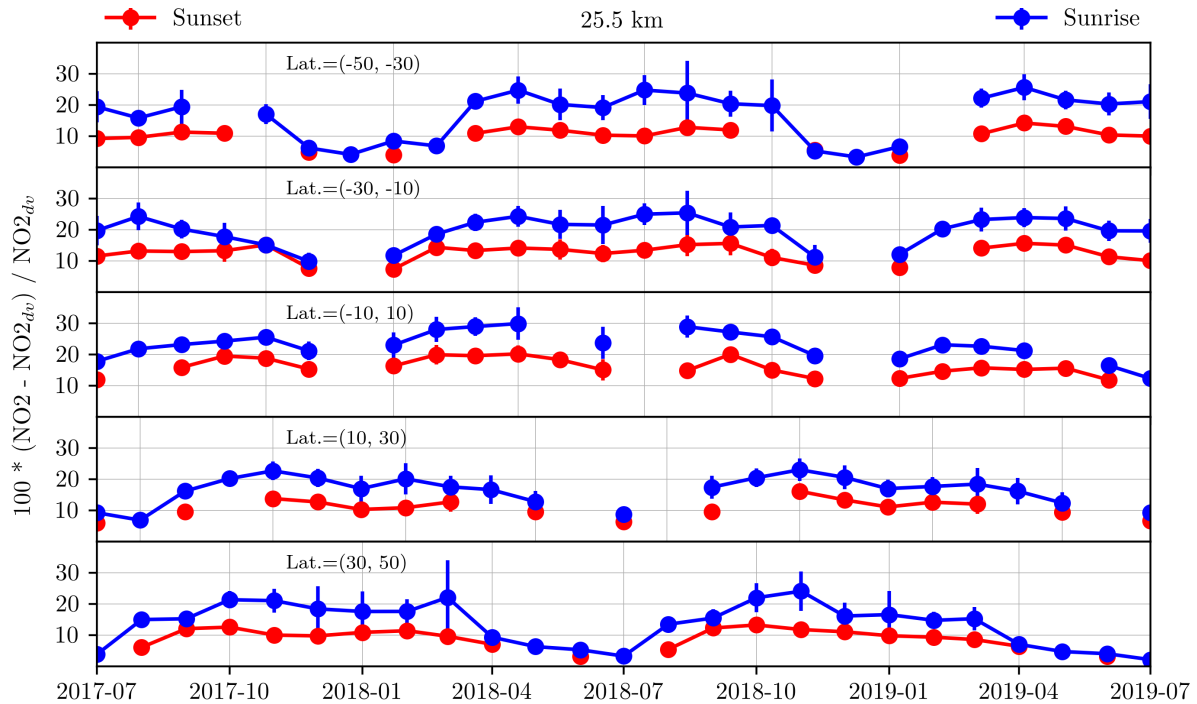


Figure 8. Mean difference between the SAGE v5.1 and diurnally varying (dv) retrievals for SAGE III/ISS sunset and sunrise NO_2 at 25.5 km. The error bars are the standard deviation.

the exact choice of coincidence criteria has minimal effect on the results. The SAGE III/ISS profiles were shifted from sunrise and sunset to the OSIRIS measurement time using PRATMO. The SAGE III/ISS NO_2 is generally biased high compared to the OSIRIS NO_2 , with a difference of up to ~~40~~50% at low altitudes/high latitudes. The differences between SAGE III/ISS and OSIRIS are within the combined uncertainties of the instruments. In general the SAGE III/ISS sunrise measurements agree better with OSIRIS than sunset, which could be because OSIRIS measures close to sunrise. The comparison was also performed excluding OSIRIS profiles with a SZA angle greater than 86° , where the diurnal effect is significant. This had a negligible effect on the difference with SAGE III/ISS.

Accounting for diurnal variations in the SAGE III/ISS retrieval improves agreement with OSIRIS by up to 20% in the mid-stratosphere (panel b of Figure 9). Overall the diurnally varying SAGE III/ISS NO_2 agrees better with the OSIRIS NO_2 than the SAGE v5.1 NO_2 . The only region where this is not true is near the tropical tropopause. This area is where the diurnal effect becomes large (Figure 7), resulting in much smaller SAGE III/ISS NO_2 values. The sunset NO_2 in particular decreases by up to 50% below 25 km in the tropics. This is larger than the initial difference between SAGE III/ISS and OSIRIS, resulting in the ~~positive~~negative bias that is observed from 15 to 25 km at low latitudes.

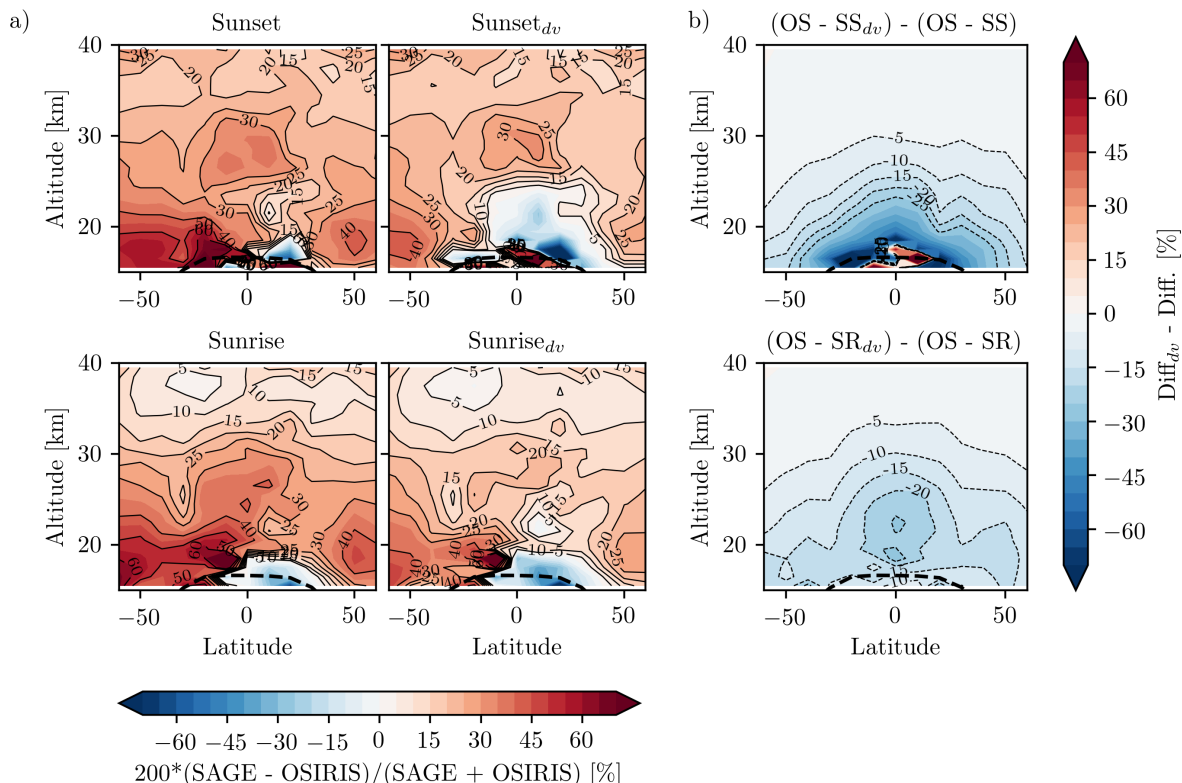


Figure 9. Panel a: Zonal mean percent differences of SAGE III/ISS sunset and sunrise NO_2 and OSIRIS NO_2 coincident measurements for the SAGE v5.1 and diurnally varying (dv) retrievals. The contour spacing is 5%. The bold dashed line is the mean tropopause location. Panel b: Difference between the columns in panel a.

215 6 Conclusions

We have developed a retrieval algorithm that uses publicly available SAGE III/ISS data to account for changes in NO_2 along the occultation line of sight that come from the photochemically driven diurnal cycle. The retrieval relies upon scaling factors derived from a photochemical box model with input ozone, temperature, and pressure profiles taken from the reported SAGE III/ISS scan.

220 It was determined that the neglect of diurnal variations in the SAGE v5.1 retrieval always biases the results high. Note that this high bias is present in NO_2 retrieved from any occultation instrument that neglects diurnal variability. In the case of SAGE III/ISS NO_2 , we found that carefully accounting for diurnal variations in the retrieval is quite important below 30 km, with an effect nearing 20% on the resulting values. The correction has the greatest effect at high winter latitudes, and is more important for sunrise occultations than sunset. These are potentially important differences in the reported NO_2 densities in the lower
 225 stratosphere, where several interesting chemical and dynamical science questions remain. Including diurnal variations in the

NO₂ retrieval also has an impact on the monthly zonal mean time series which should be considered when studying long term variability.

Accounting for these diurnal variations in the SAGE III/ISS retrieval improves the agreement ~~between~~ with OSIRIS NO₂ by up to 20% at lower altitudes. While there is a remaining bias between SAGE III/ISS and OSIRIS that is not well understood, it
230 has a reasonable magnitude considering the very different measurement and retrieval techniques, and is within their combined uncertainties.

Data availability. The SAGE III/ISS Level 1 and 2 data are available through <https://search.earthdata.nasa.gov/>. The SAGE III/ISS NO₂ that was retrieved by accounting for diurnal variations is available at <https://research-groups.usask.ca/osiris/data-products.php>. OSIRIS NO₂ is also available at the previous link.

235 *Author contributions.* KD performed the analysis and prepared the manuscript. DZ assisted with writing the retrieval code. AB and DD proposed the original idea for the project and provided guidance throughout. RD provided assistance with using the SAGE III/ISS data. DF and WR, along with the other authors, provided significant feedback on the analysis and the manuscript.

Competing interests. The authors declare that they have no conflicts of interest.

Acknowledgements. The authors thanks the Swedish National Space Agency and the Canadian Space Agency for the continued operation
240 and support of Odin-OSIRIS. We also thank the SAGE III/ISS science team for providing the SAGE III/ISS data. SAGE III/ISS is a NASA Langley managed Mission funded by the NASA Science Mission Directorate within the Earth Systematic Mission Program. Enabling partners are the NASA Human Exploration and Operations Mission Directorate, International Space Station Program and the European Space Agency. The National Center for Atmospheric Research is sponsored by the US National Science Foundation.

References

- 245 Adams, C., Bourassa, A. E., McLinden, C. A., Sioris, C. E., von Clarmann, T., Funke, B., Rieger, L. A., and Degenstein, D. A.: Effect of volcanic aerosol on stratospheric NO₂ and N₂O₅ from 2002–2014 as measured by Odin-OSIRIS and Envisat-MIPAS, *Atmospheric Chemistry and Physics*, 17, 8063–8080, <https://doi.org/10.5194/acp-17-8063-2017>, 2017.
- Bourassa, A. E., McLinden, C. A., Sioris, C. E., Brohede, S., Bathgate, A. F., Llewellyn, E. J., and Degenstein, D. A.: Fast NO₂ retrievals from Odin-OSIRIS limb scatter measurements, *Atmospheric Measurement Techniques*, 4, 965–972, <https://doi.org/10.5194/amt-4-965-2011>,
250 <https://www.atmos-meas-tech.net/4/965/2011/>, 2011.
- Brohede, S. M., Haley, C. S., McLinden, C. A., Sioris, C. E., Murtagh, D. P., Petelina, S. V., Llewellyn, E. J., Bazureau, A., Goutail, F., Randall, C. E., et al.: Validation of Odin/OSIRIS stratospheric NO₂ profiles, *Journal of Geophysical Research: Atmospheres*, 112, 2007.
- Cisewski, M., Zawodny, J., Gasbarre, J., Eckman, R., Topiwala, N., Rodriguez-Alvarez, O., Cheek, D., and Hall, S.: The Stratospheric Aerosol and Gas Experiment (SAGE III) on the International Space Station (ISS) Mission, in: *Sensors, Systems, and Next-Generation Satellites XVIII*, vol. 9241, p. 924107, International Society for Optics and Photonics, 2014.
255
- Dubé, K., Randel, W., Bourassa, A., Zawada, D., McLinden, C., and Degenstein, D.: Trends and Variability in Stratospheric NO_x Derived From Merged SAGE II and OSIRIS Satellite Observations, *Journal of Geophysical Research: Atmospheres*, 125, e2019JD031 798, 2020.
- Galytska, E., Rozanov, A., Chipperfield, M. P., Dhomse, Weber, M., Arosio, C., Feng, W., and Burrows, J. P.: Dynamically controlled ozone decline in the tropical mid-stratosphere observed by SCIAMACHY, *Atmospheric Chemistry and Physics*, 19, 767–783,
260 <https://doi.org/10.5194/acp-19-767-2019>, <https://www.atmos-chem-phys.net/19/767/2019/>, 2019.
- Gordley, L., Russell III, J., Mickley, L., Frederick, J., Park, J., Stone, K., Beaver, G., McInerney, J., Deaver, L., Toon, G., et al.: Validation of nitric oxide and nitrogen dioxide measurements made by the Halogen Occultation Experiment for UARS platform, *Journal of Geophysical Research: Atmospheres*, 101, 10 241–10 266, 1996.
- Haley, C. S., Brohede, S. M., Sioris, C. E., Griffioen, E., Murtagh, D. P., McDade, I. C., Eriksson, P., Llewellyn, E. J., Bazureau, A.,
265 and Goutail, F.: Retrieval of stratospheric O₃ and NO₂ profiles from Odin Optical Spectrograph and Infrared Imager System (OSIRIS) limb-scattered sunlight measurements, *Journal of Geophysical Research: Atmospheres*, 109, <https://doi.org/10.1029/2004JD004588>, <https://agupubs.onlinelibrary.wiley.com/doi/abs/10.1029/2004JD004588>, 2004.
- Liley, J. B., Johnston, P. V., McKenzie, R. L., Thomas, A. J., and Boyd, I. S.: Stratospheric NO₂ variations from a long time series at Lauder, New Zealand, *Journal of Geophysical Research: Atmospheres*, 105, 11 633–11 640, <https://doi.org/10.1029/1999JD901157>, <https://agupubs.onlinelibrary.wiley.com/doi/abs/10.1029/1999JD901157>,
270
- Llewellyn, E. J., Lloyd, N. D., Degenstein, D. A., Gattinger, R. L., Petelina, S. V., Bourassa, A. E., Wiensz, J. T., Ivanov, E. V., McDade, I. C., Solheim, B. H., McConnell, J. C., Haley, C. S., von Savigny, C., Sioris, C. E., McLinden, C. A., Griffioen, E., Kaminski, J., Evans, W. F., Puckrin, E., Strong, K., Wehrle, V., Hum, R. H., Kendall, D. J., Matsushita, J., Murtagh, D. P., Brohede, S., Stegman, J., Witt, G., Barnes, G., Payne, W. F., Piché, L., Smith, K., Warshaw, G., Deslauniers, D. L., Marchand, P., Richardson, E. H., King, R. A., Wevers,
275 I., McCreath, W., Kyrölä, E., Oikarinen, L., Leppelmeier, G. W., Auvinen, H., Mégie, G., Hauchecorne, A., Lefèvre, F., de La Nöe, J., Ricaud, P., Frisk, U., Sjöberg, F., von Schéele, F., and Nordh, L.: The OSIRIS instrument on the Odin spacecraft, *Canadian Journal of Physics*, 82, 411–422, <https://doi.org/10.1139/p04-005>, 2004.
- Mauldin III, L. E., Salikhov, R., Habib, S., Vladimirov, A. G., Carraway, D., Petrenko, G., and Comella, J.: Meteor-3M (1)/Stratospheric Aerosol and Gas Experiment III (SAGE III) jointly sponsored by the National Aeronautics and Space Administration and the Russian

- 280 Space Agency, in: *Optical Remote Sensing of the Atmosphere and Clouds*, vol. 3501, pp. 355–365, International Society for Optics and Photonics, 1998.
- McCormick, M.: Sage II: An overview, *Advances in Space Research*, 7, 219 – 226, [https://doi.org/https://doi.org/10.1016/0273-1177\(87\)90151-7](https://doi.org/https://doi.org/10.1016/0273-1177(87)90151-7), <http://www.sciencedirect.com/science/article/pii/0273117787901517>, 1987.
- McLinden, C. A., Olsen, S. C., Hannegan, B., Wild, O., Prather, M. J., and Sundet, J.: Stratospheric ozone in 3-D models: A simple chemistry and the cross-tropopause flux, *Journal of Geophysical Research: Atmospheres*, 105, 14 653–14 665, <https://doi.org/10.1029/2000JD900124>, 2000.
- 285 McLinden, C. A., Haley, C. S., and Sioris, C. E.: Diurnal effects in limb scatter observations, *Journal of Geophysical Research: Atmospheres*, 111, 2006.
- Murtagh, D., Frisk, U., Merino, F., Ridal, M., Jonsson, A., Stegman, J., Witt, G., Eriksson, P., Jiménez, C., Megie, G., Noë, J. d. I., Ricaud, P., Baron, P., Pardo, J. R., Hauchcorne, A., Llewellyn, E. J., Degenstein, D. A., Gattinger, R. L., Lloyd, N. D., Evans, W. F., McDade, I. C., Haley, C. S., Sioris, C., Savigny, C. v., Solheim, B. H., McConnell, J. C., Strong, K., Richardson, E. H., Leppelmeier, G. W., Kyrölä, E., Auvinen, H., and Oikarinen, L.: An overview of the Odin atmospheric mission, *Canadian Journal of Physics*, 80, 309–319, <https://doi.org/10.1139/p01-157>, <https://doi.org/10.1139/p01-157>, 2002.
- 290 Newchurch, M. J., Allen, M., Gunson, M. R., Salawitch, R. J., Collins, G. B., Huston, K. H., Abbas, M. M., Abrams, M. C., Chang, A. Y., Fahey, D. W., Gao, R. S., Irion, F. W., Loewenstein, M., Manney, G. L., Michelsen, H. A., Podolske, J. R., Rinsland, C. P., and Zander, R.: Stratospheric NO and NO₂ abundances from ATMOS Solar-Occultation Measurements, *Geophysical Research Letters*, 23, 2373–2376, <https://doi.org/10.1029/96GL01196>, <https://agupubs.onlinelibrary.wiley.com/doi/abs/10.1029/96GL01196>, 1996.
- 295 Park, M., Randel, W. J., Kinnison, D. E., Bourassa, A. E., Degenstein, D. A., Roth, C. Z., McLinden, C. A., Sioris, C. E., Livesey, N. J., and Santee, M. L.: Variability of Stratospheric Reactive Nitrogen and Ozone Related to the QBO, *Journal of Geophysical Research: Atmospheres*, 122, 10,103–10,118, <https://doi.org/10.1002/2017JD027061>, 2017.
- 300 Prather, M. J.: Catastrophic loss of stratospheric ozone in dense volcanic clouds, *Journal of Geophysical Research: Atmospheres*, 97, 10 187–10 191, <https://doi.org/10.1029/92JD00845>, <https://agupubs.onlinelibrary.wiley.com/doi/abs/10.1029/92JD00845>, 1992.
- Randel, W. J., Wu, F., Russell III, J. M., and Waters, J.: Space-time patterns of trends in stratospheric constituents derived from UARS measurements, *Journal of Geophysical Research: Atmospheres*, 104, 3711–3727, <https://doi.org/10.1029/1998JD100044>, <https://agupubs.onlinelibrary.wiley.com/doi/abs/10.1029/1998JD100044>, 1999.
- 305 Rieger, L. A., Zawada, D. J., Bourassa, A. E., and Degenstein, D. A.: A Multiwavelength Retrieval Approach for Improved OSIRIS Aerosol Extinction Retrievals, *Journal of Geophysical Research: Atmospheres*, 124, 7286–7307, <https://doi.org/10.1029/2018JD029897>, <https://agupubs.onlinelibrary.wiley.com/doi/abs/10.1029/2018JD029897>, 2019.
- Russell III, J. M., Gordley, L. L., Park, J. H., Drayson, S. R., Hesketh, W. D., Cicerone, R. J., Tuck, A. F., Frederick, J. E., Harries, J. E., and Crutzen, P. J.: The Halogen Occultation Experiment, *Journal of Geophysical Research: Atmospheres*, 98, 10 777–10 797, <https://doi.org/10.1029/93JD00799>, <https://agupubs.onlinelibrary.wiley.com/doi/abs/10.1029/93JD00799>, 1993.
- SAGE III Algorithm Theoretical Basis Document, T.: SAGE III Algorithm Theoretical Basis Document (ATBD) Solar and Lunar Algorithm, Tech. rep., LaRC 475-00-109, <https://eosps0.gsfc.nasa.gov/sites/default/files/atbd/atbd-sage-solar-lunar.pdf>, 2002.
- 315 Sioris, C. E., Rieger, L. A., Lloyd, N. D., Bourassa, A. E., Roth, C. Z., Degenstein, D. A., Camy-Peyret, C., Pfeilsticker, K. E., Berthet, G., Catoire, V., Goutail, F., Pommereau, J.-P., and McLinden, C. E.: Improved OSIRIS NO₂ retrieval algorithm: description and validation, *Atmospheric Measurement Techniques*, 10, 1155 – 1168, <https://doi.org/10.5194/amt-10-1155-2017>, 2017.